Products of the Gas-Phase Reactions of the OH Radical with 1-Methoxy-2-propanol and 2-Butoxyethanol

ARTICLE *in* ENVIRONMENTAL SCIENCE AND TECHNOLOGY · SEPTEMBER 1998

Impact Factor: 5.33 · DOI: 10.1021/es980455c

3 AUTHORS, INCLUDING:

Sara M Aschmann
University of California, Riverside
200 PUBLICATIONS **7,389** CITATIONS
SEE PROFILE

Roger Atkinson
University of California, Riverside
531 PUBLICATIONS **29,616** CITATIONS
SEE PROFILE

Environ. Sci. Technol. **1998**, *32,* 3336−3345

Products of the Gas-Phase Reactions of the OH Radical with 1-Methoxy-2-propanol and 2-Butoxyethanol

ERNESTO C. TUAZON, SARA M. ASCHMANN, AND ROGER ATKINSON*,†

Air Pollution Research Center, University of California, Riverside, California 92521

Glycol ethers are used as solvents and are hence liable to be released to the atmosphere, where they react and contribute to the formation of photochemical air pollution. In this work, products of the gas-phase reactions of the OH radical with 1-methoxy-2-propanol and 2-butoxyethanol in the presence of NO have been investigated at 298 ± 2 K and 740 Torr total pressure of air by gas chromatography, in situ Fourier transform infrared spectroscopy, and in situ atmospheric pressure ionization tandem mass spectrometry. The products observed from 1-methoxy-2-propanol were methyl formate, methoxyacetone, and acetaldehyde with molar formation yields of 0.59 ± 0.05, 0.39 ± 0.04, and 0.56 ± 0.07, respectively. The products observed and quantified from 2-butoxyethanol were *n*-butyl formate, 2-hydroxyethyl formate, propanal, 3-hydroxybutyl formate, and an organic nitrate (attributed to $CH_3CH_2CH_2CH_2OCH(ONO_2)CH_2OH$ and its isomers), with molar formation yields of 0.57 ± 0.05, 0.22 ± 0.05, 0.21 ± 0.02, 0.07 ± 0.03, and 0.10 ± 0.03, respectively. An additional product of molecular weight 132, attributed to one or more hydroxycarbonyl products, was also observed from the 2-butoxyethanol reaction by atmospheric pressure ionization mass spectrometry. For both glycol ethers, the majority of the reaction products and reaction pathways are accounted for, and detailed reaction mechanisms are presented which account for the observed products.

Introduction

Volatile organic compounds present in the atmosphere can undergo photolysis and chemical reaction with OH radicals, NO_3 radicals, and O_3 (*1, 2*), with the OH radical reaction being an important, and often dominant, atmospheric loss process (*1, 2*). Glycol ethers are used as solvents (*3, 4*) and are hence liable to be released into the atmosphere where they may contribute to the formation of photochemical air pollution in urban and regional areas (*5*). Glycol ethers react with OH radicals (*6*−*12*) and NO_3 radicals (*12, 13*), with the OH radical reactions being calculated to be the dominant tropospheric loss process and with calculated lifetimes of approximately 1 day or less (*11, 12*). However, to date there have been few reported studies of the products and mechanisms of the OH radical-initiated reactions of glycol ethers, with product studies having been reported for 2-ethoxyethanol (*14*) and 2-butoxyethanol (*15*). As part of an overall study of the tropospheric chemistry of the glycol ethers 1-methoxy-2-propanol [$CH_3CH(OH)CH_2OCH_3$] and 2-butoxyethanol [$CH_3CH_2CH_2CH_2OCH_2CH_2OH$], we have investigated the products of the reactions of these two glycol ethers with OH radicals in the presence of NO. The kinetics of the reactions of 1-methoxy-2-propanol and 2-butoxyethanol with OH radicals, NO_3 radicals, and O_3 have been reported elsewhere (*12*).

Experimental Section

Experiments were carried out at 298 ± 2 K and 740 Torr total pressure of air in a 5870-L evacuable, Teflon-coated chamber containing an in situ multiple reflection optical system interfaced to a Nicolet 7199 Fourier transform infrared (FT-IR) absorption spectrometer and with irradiation provided by a 24 kW xenon arc filtered through a 0.25 in. thick Pyrex pane (to remove wavelengths <300 nm); in a 7900-L Teflon chamber with analysis by gas chromatography with flame ionization detection (GC-FID) and combined gas chromatography−mass spectrometry (GC-MS), with irradiation provided by two parallel banks of blacklamps; and in a 7500-L Teflon chamber interfaced to a PE SCIEX API III MS/MS direct air sampling, atmospheric pressure ionization tandem mass spectrometer (API-MS), again with irradiation provided by two parallel banks of blacklamps. All three chambers are fitted with Teflon-coated fans to ensure rapid mixing of reactants during their introduction into the chamber.

Hydroxyl radicals were generated in the presence of NO by the photolysis of methyl nitrite (CH_3ONO) in air at wavelengths >300 nm (*12,16*):

$$CH_3ONO + h\nu \rightarrow CH_3O^{\bullet} + NO \quad (1)$$

$$CH_3O^{\bullet} + O_2 \rightarrow HCHO + HO_2 \quad (2)$$

$$HO_2 + NO \rightarrow OH + NO_2 \quad (3)$$

and NO was added to the reactant mixtures to suppress the formation of O_3 and hence of NO_3 radicals.

Teflon Chamber with Analysis by GC-FID. For the experiments carried out in the 7900-L Teflon chamber (at ∼5% relative humidity), the initial reactant concentrations (in units of molecules per cubic centimeter, molecule cm^{-3}) were CH_3ONO, (2.2−2.3) × 10^{14}; NO, (1.9−2.3) × 10^{14}; and 1-methoxy-2-propanol, (2.27−2.36) × 10^{13}, or 2-butoxyethanol, (2.25−2.55) × 10^{13}. [Note that 1 part per million (ppm) mixing ratio = 2.40 × 10^{13} molecule cm^{-3} at 298 K and 740 Torr total pressure.] Irradiations were carried out at 20% of the maximum light intensity for 4−15 min (1-methoxy-2-propanol) or 3−12 min (2-butoxyethanol), resulting in up to 52% and 59% reaction of the initial 1-methoxy-2-propanol and 2-butoxyethanol, respectively. The concentrations of the glycol ethers and selected products were measured during the experiments by GC-FID. Gas samples of 100 cm^3 were collected from the chamber onto Tenax-TA solid adsorbent, with subsequent thermal desorption at ∼225 °C onto a DB-1701 megabore column in a Hewlett-Packard (HP) 5710 GC, initially held at −40, −20, or 0 °C, depending on the products to be analyzed, and then temperature programmed to 200 °C at 8 °C min^{-1}. Gas samples were also collected from the chamber onto Tenax-TA solid adsorbent for thermal desorption with analysis by GC-MS, using a 50 m HP-5 fused

* Corresponding author e-mail: ratkins@mail.vcr.edu; phone: (909)787-4191; fax: (909)787-5004.

† Also Interdepartmental Program in Environmental Toxicology, Department of Environmental Sciences, and Department of Chemistry.

S0013-936X(98)00455-6 CCC: $15.00
Published on Web 09/15/1998

silica capillary column in an HP 5890 GC interfaced to a HP 5971 mass selective detector operating in the scanning mode. GC-FID response factors were determined as previously described (*17*).

Evacuable Chamber Experiments with FT-IR Analysis. For the experiments carried out in the 5870-L evacuable, Teflon-coated chamber (at <1% relative humidity), the initial concentrations for all runs were 2.5×10^{14} molecule cm^{-3} each of CH_3ONO, NO, and 1-methoxy-2-propanol or 2-butoxyethanol. Vapors of 1-methoxy-2-propanol, methyl nitrite, and nitric oxide were measured by a capacitance manometer (MKS Baratron, 100 Torr sensor) into calibrated 5 and 2-L Pyrex bulbs and introduced into the chamber by flushing the contents of the bulbs with N_2 gas. Vapors of 2-butoxyethanol were introduced into the chamber by heating a weighed amount of the liquid sample and flushing with a stream of heated N_2 gas. IR spectra of the reaction mixtures were recorded prior to and during irradiation with 64 scans (corresponding to 2.0-min averaging time) per spectrum, a full-width-at-half-maximum resolution of 0.7 cm^{-1}, and a path length of 62.9 m (*16, 18*). The mixtures were irradiated continuously for a 33−38-min period with FT-IR monitoring every 2−4 min. One experiment with a 1-methoxy-2-propanol−CH_3ONO−NO−air mixture was carried out with concurrent FT-IR and GC-FID measurements and employed intermittent irradiation to allow for GC sampling during the intervening dark periods.

Teflon Chamber with Analysis by API-MS. In the experiments with API-MS analyses, the chamber contents were sampled through a 25-mm-diameter × 75-cm-length Pyrex tube at ~20 L min^{-1} directly into the API mass spectrometer source. The operation of the API-MS in the MS (scanning) and MS/MS [with collision activated dissociation (CAD)] modes has been described elsewhere (*19*). Use of the MS/MS mode with CAD allows the "daughter ion" or "parent ion" spectrum of a given ion peak observed in the MS scanning mode to be obtained (*19*). The positive ion mode was used in these API-MS and API-MS/MS analyses, with protonated water hydrates ($H_3O^+(H_2O)_n$) generated by the corona discharge in the chamber diluent gas being responsible for the protonation of analytes. Ions are drawn by an electric potential from the ion source through the sampling orifice into the mass-analyzing first quadrupole or third quadrupole. For these experiments, the API-MS instrument was operated under conditions that favored the formation of dimer ions in the ion source region (*19*). Neutral molecules and particles are prevented from entering the orifice by a flow of high-purity nitrogen ("curtain" gas), and as a result of the declustering action of the curtain gas on the hydrated ions, the ions that are mass-analyzed are mainly protonated molecular ions ($[M+H]^+$) and their protonated homo- and heterodimers (*19*). The initial concentrations of CH_3ONO, NO, and 1-methoxy-2-propanol or 2-butoxyethanol were ~4.8×10^{13} molecule cm^{-3} each, and irradiations were carried out for 5 min at 20% of the maximum light intensity, resulting in a 33% reaction of the initially present 1-methoxy-2-propanol (as measured by GC-FID) and a 40−45% reaction of the initially present 2-butoxyethanol (estimated from the 1-methoxy-2-propanol experiment carried out with similar initial CH_3ONO and NO concentrations and light intensity, and hence a similar OH radical concentration).

Chemicals. The chemicals used, and their stated purities (in parentheses), were acetaldehyde (99.5+%), butanal (99%), 2-butoxyethanol (99+%), *n*-butyl formate (97%), methoxyacetone (97%), 1-methoxy-2-propanol (98%), methyl formate (99%), propanal (97%), and *n*-propyl nitrate (97%), Aldrich Chemical Co.; and NO (≥ 99.0%), Matheson Gas Products. Methyl nitrite was prepared as described by Taylor et al. (*20*).

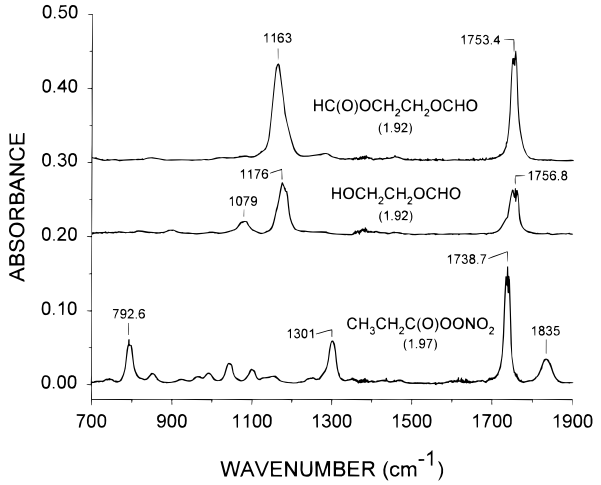

FIGURE 1. IR spectra of ethylene glycol diformate, 2-hydroxyethyl formate, and peroxypropionyl nitrate (PPN). The numbers in parentheses are equivalent concentrations in units of 10^{13} molecule cm^{-3} for a 62.9-m path length (see text).

Peroxypropionyl nitrate [$CH_3CH_2C(O)OONO_2$; PPN] was prepared from the Cl atom-initiated photooxidation of propanal in the presence of NO_2 [with initial concentrations (in units of 10^{14} molecule cm^{-3}) of propanal, 2.46; NO_2, 1.61; and Cl_2, 9.84]. The spectrum of PPN was derived from that of the reaction mixture by spectral desynthesis [stepwise subtraction of absorptions by known components (*16*)]. The calibration obtained, based on the amount of propanal which reacted during the early part of the photolysis (≤15% reaction), was in good agreement with the IR absorptivities published by Stephens (*21*), and an infrared spectrum of peroxypropionyl nitrate is presented in Figure 1.

2-Hydroxyethyl formate [ethylene glycol monoformate; $HOCH_2CH_2OCHO$] was prepared by room-temperature, acid-catalyzed reaction of formic acid with a 20-fold excess of ethylene glycol. The reaction mixture was extracted with benzene and, with IR spectroscopic monitoring of the vapors sampled in a 25-cm path length cell, top fractions were successively discarded in a vacuum line until the absorption bands of benzene, water vapor, and formic acid were no longer detectable. From a middle fraction of the remaining liquid, vapor samples were obtained which were mixtures of 2-hydroxyethyl formate and ethylene glycol diformate of varying concentration ratios but with no detectable ethylene glycol component. Continued extraction of the unequilibriated vapor above the liquid sample ultimately yielded only vapors of the diformate, thus allowing quantitative IR spectra of ethylene glycol diformate to be recorded. This, therefore, enabled quantitative spectra of 2-hydroxyethyl formate to be derived from its mixtures with the diformate. For example, three successive vapor samples from a separate preparation were found to contain 69%, 81%, and 89% 2-hydroxyethyl formate, based on the measured pressures of the vapor samples and the calibrated IR reference spectrum of ethylene glycol diformate. An iterative spectral subtraction, initially based on the 1163 cm^{-1} band of the diformate, allowed the distinct spectrum of the monoformate to be revealed and derived from that of the two-component mixture, and calibrated spectra of both compounds are shown in Figure 1. Individual analyses of consecutive vapor samples from the monoformate preparation were essential in obtaining the above calibrations, since the liquid fraction underwent changes in composition upon prolonged standing at room temperature because of the tendency to reestablish an equilibrium composition between the monoformate, diformate, and ethylene glycol (*14*). The distinct 1756.8 cm^{-1} band of 2-hydroxyethyl formate vapor shown in Figure 1

was verified to have an exact correspondence in contour and position with that of a product formed during photolysis of a $CH_3OCH_2CH_2OH-Cl_2$–air mixture, where $HOCH_2CH_2OCHO$ is one of the expected products.

3-Hydroxybutyl formate was prepared in a mixture with its coproducts 3-hydroxy-1-methylpropyl formate and 1,3-butanediol diformate by the acid-catalyzed reaction of formic acid with a 10-fold excess of 1,3-butanediol and subsequent benzene extraction of the mixture. A benzene extract of the reaction mixture was fractionated in a vacuum line as described above for 2-hydroxyethyl formate. Vapor samples were extracted which contained only a mixture of formates, as indicated by two dominant IR absorption bands at 1184 and 1747 cm^{-1}, but further fractionation of the components could not be achieved. The gas chromatogram of a liquid sample injected into the 5870-L chamber showed four peaks with retention times later than that of 2-butoxyethanol (also added to the mixture as a retention time marker) by 1.53, 1.86, 2.07 and 2.61 min, with the first peak corresponding to 41% (by weight) of 1,3-butanediol, and with the other three peaks corresponding, respectively, to 3-hydroxybutyl formate, 3-hydroxy-1-methylpropyl formate, and 1,3-butanediol diformate. The GC peak at 1.86 min beyond that of 2-butoxyethanol was the only one which corresponded to GC peaks in GC-FID analyses of irradiated $CH_3ONO-NO-$2-butoxyethanol–air mixtures and was the basis of the assignment to 3-hydroxybutyl formate and, hence, of the other two peaks. The relative molar fractions of the three components were calculated from the GC peak areas using their calculated Effective Carbon Numbers (ECNs) (*22*), and for the above liquid sample were 0.66, 0.27, and 0.07 for 3-hydroxybutyl formate, 3-hydroxy-1-methylpropyl formate, and 1,3-butanediol diformate, respectively. The GC response factor for 3-hydroxybutyl formate obtained from these analyses of weighed liquid sample injections was in excellent agreement with an average of the response factors obtained relative to the measured response factors for 2-butoxyethanol and *n*-butyl formate using the calculated ECNs for 2-butoxyethanol, *n*-butyl formate and 3-hydroxybutyl formate (*22*).

2-Hydroxybutyl formate was synthesized by an analogous procedure from 1,2-butanediol, and GC-FID analyses of the synthesized mixture (again with added 2-butoxyethanol as a retention time marker) showed GC peaks with retention times 0.70, 1.42, and 2.18 min later than that of 2-butoxyethanol, with the first of these being 1,2-butanediol. These GC-FID analyses show that 2-hydroxybutyl formate and 3-hydroxybutyl formate do not coelute on the DB-1701 column used here.

Results

Teflon Chamber with Analysis by GC-FID. GC-FID and GC-MS analyses of irradiated $CH_3ONO-NO-$1-methoxy-2-propanol–air and $CH_3ONO-NO-$2-butoxyethanol–air mixtures showed, by matching of GC retention times and (apart from 2-hydroxyethyl formate and 3-hydroxybutyl formate) mass spectra with those of authentic standards, the formation of methyl formate [CH_3OCHO], acetaldehyde and methoxyacetone [$CH_3C(O)CH_2OCH_3$] from 1-methoxy-2-propanol, and *n*-butyl formate, propanal, 2-hydroxyethyl formate, and 3-hydroxybutyl formate from 2-butoxyethanol. Because of difficulties in obtaining a measured GC-FID response factor for 2-hydroxyethyl formate, this product was not quantified from the GC-FID analyses (see FT-IR data below). It should be noted, however, that using a GC-FID response factor obtained from the calculated ECN for 2-hydroxyethyl formate (*22*) resulted in a 2-hydroxyethyl formate formation yield in good agreement with that determined by FT-IR spectroscopic analyses. One of the peaks in the GC-FID analyses of the synthesized 2-hydroxybutyl formate–1-hydroxymethyl-propyl formate mixture was within ~0.06 min of a product peak from the irradiated $CH_3ONO-NO-$2-butoxyethanol–air mixtures, and we use this GC-FID peak to derive an upper limit for the 2-hydroxybutyl formate formation yield.

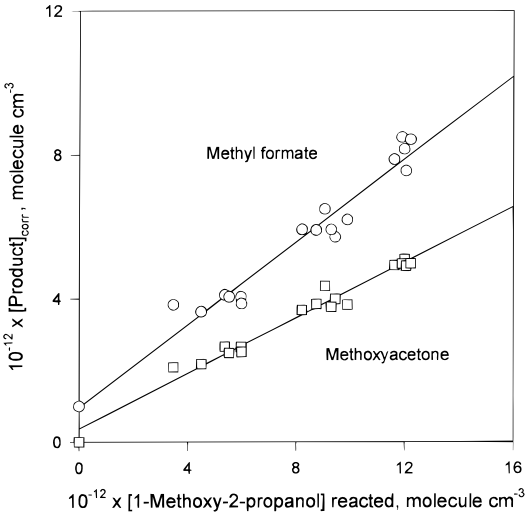

FIGURE 2. Plots of the amounts of methyl formate and methoxyacetone formed, corrected for reactions with the OH radical, against the amounts of 1-methoxy-2-propanol reacted with the OH radical in the presence of NO, with analyses by GC-FID. The data for methyl formate have been displaced vertically by 1×10^{12} molecule cm^{-3} for clarity.

The products observed and quantified also react with the OH radical (*1, 2, 23*), and hence secondary reactions of the products with the OH radical were taken into account as described previously (*24*) using OH radical reaction rate constants of (in units of 10^{-12} cm^3 $molecule^{-1}$ s^{-1}) 1-methoxy-2-propanol, 20.9 (*12*); 2-butoxyethanol, 29.4 (*12*); acetaldehyde, 15.8 (*1*); propanal, 19.6 (*1*); butanal, 23.5 (*1*); methyl formate, 0.200 (*25, 26*); methoxyacetone, 6.8 (*8*); *n*-butyl formate, 3.33 (*25, 26*); 2-hydroxybutyl formate, 13.6 [estimated] (*27*); and 3-hydroxybutyl formate, 11.9 [estimated] (*27*). The multiplicative correction factors *F* to take into account secondary reactions increase with the rate constant ratio $k(OH + product)/k(OH + reactant)$ and with the extent of reaction (*24*). The maximum values of *F* were 1.35 for acetaldehyde, <1.01 for methyl formate, and 1.14 for methoxyacetone formation from 1-methoxy-2-propanol, and were 1.06 for *n*-butyl formate, 1.43 for butanal, 1.35 for propanal, 1.25 for 2-hydroxybutyl formate, and 1.22 for 3-hydroxybutyl formate formation from 2-butoxyethanol.

Figure 2 shows representative plots of the amounts of methyl formate and methoxyacetone formed, corrected for reaction with the OH radical, against the amounts of 1-methoxy-2-propanol reacted, and Figure 3 shows similar plots for the formation of *n*-butyl formate and propanal from 2-butoxyethanol. The formation yields of the products quantified as obtained by least-squares analyses of plots such as those shown in Figures 2 and 3 are given in Table 1 (which also contains an upper limit to the formation yield for butanal). Two independent sets of experiments were carried out to measure the formation yields of methyl formate and methoxyacetone from the 1-methoxy-2-propanol reaction and, as shown in Table 1, the agreement between the two measured methyl formate and methoxyacetone formation yields is excellent.

Evacuable Chamber Experiments with FT-IR Analysis. In situ FT-IR spectroscopic analyses of irradiated $CH_3ONO-NO-$1-methoxy-2-propanol–air mixtures showed the formation of methyl formate, acetaldehyde, and methoxyacetone as the major products. The formation of these products, together with peroxyacetyl nitrate (PAN), in the

TABLE 1. Products and Their Formation Yields Observed from the Reactions of the OH Radical with 1-Methoxy-2-propanol and 2-Butoxyethanol in the Presence of NO at 298 ± 2 K and 740 Torr Total Pressure of Air

		formation yield	
glycol ether	product	GC-FID[a]	FT-IR[b]
1-methoxy-2-propanol	methyl formate	0.579 ± 0.078[c] 0.569 ± 0.079[c] 0.58 ± 0.08[d]	0.59 ± 0.05
	acetaldehyde	0.49 ± 0.13	0.58 ± 0.08[e]
	methoxyacetone	0.396 ± 0.056[c] 0.399 ± 0.039[c] 0.39 ± 0.05[d]	0.39 ± 0.05
2-butoxyethanol	*n*-butyl formate	0.55 ± 0.06	0.60 ± 0.07
	butanal	<0.01	
	propanal	0.21 ± 0.02	0.21 ± 0.08[e]
	2-hydroxyethyl formate		0.22 ± 0.05
	3-hydroxybutyl formate	0.07 ± 0.03	
	2-hydroxybutyl formate	<0.03	
	organic nitrate		0.10 ± 0.03[e]

[a] Indicated errors are two least-squares standard deviations combined with estimated overall uncertainties in the GC-FID response factors for the glycol ethers and products of ±5% each, except for 3-hydroxybutyl formate for which the uncertainty in the response factor is estimated to be ±30%. [b] Indicated errors are two least-squares standard deviations combined with the estimated errors arising from the measurement uncertainties of the glycol ethers and products; i.e., ±6% for 1-methoxy-2-propanol, 2-butoxyethanol, and methoxyacetone; ±3% for methyl formate; and ±15% for 2-hydroxyethyl formate. [c] Independent sets of experiments, each with separately measured GC-FID calibration factors. [d] For combined data sets. [e] See text.

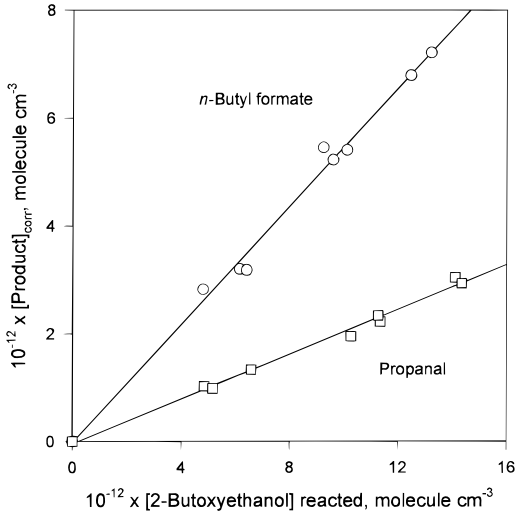

FIGURE 3. Plots of the amounts of *n*-butyl formate and propanal formed, corrected for reactions with the OH radical, against the amounts of 2-butoxyethanol reacted with the OH radical in the presence of NO, with analyses by GC-FID.

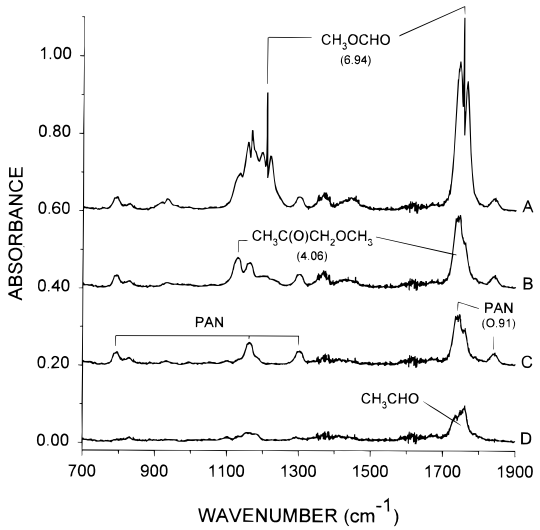

FIGURE 4. (A) Product spectrum from the photolysis of a 1-methoxy-2-propanol−CH_3ONO−NO−air mixture after 25 min of irradiation and 47% conversion of the initial 2.46 × 10^{14} molecule cm^{-3} of 1-methoxy-2-propanol, absorption byproducts from CH_3ONO and NO subtracted, (B) after subtraction of absorptions by methyl formate, (C) after subtraction of absorptions by methoxyacetone, and (D) after subtraction of absorptions by peroxyacetyl nitrate (PAN). The numbers in parentheses are concentrations in units of 10^{13} molecule cm^{-3}.

irradiated mixture is evident in the series of IR spectra presented in Figure 4, where absorptions by the remaining reactants and by the products arising primarily from the photooxidation of CH_3ONO and NO (i.e., NO_2, HNO_3, HONO, HCHO, HC(O)OH, and CH_3ONO_2) have been subtracted for clarity. Although the acetaldehyde absorption band at 1746 cm^{-1} is qualitatively seen in the product spectra (Figure 4D), its intensity is relatively weak and could not be reliably subtracted from an unknown residual band. Measurements of acetaldehyde by GC-FID in a specific experiment are described below.

Figure 5 shows plots of the methyl formate and methoxyacetone concentrations (combined data from two experiments), corrected for reaction with the OH radical, against the amounts of 1-methoxy-2-propanol reacted. The maximum values of the multiplicative factor *F* to correct for secondary reactions of the products with the OH radical during a 38-min irradiation were <1.01 and 1.17 for methyl formate and methoxyacetone, respectively. Least-squares analyses of these data lead to the methyl formate and methoxyacetone formation yields given in Table 1.

Although acetaldehyde data were not obtained from these particular experiments, an additional experiment with intermittent irradiation (see Experimental Section) was carried out which employed both FT-IR and GC-FID analyses, with acetaldehyde being quantified by GC-FID. The FT-IR analyses of 1-methoxy-2-propanol and the GC-FID analyses of acetaldehyde resulted in acetaldehyde formation yields, corrected for reaction with the OH radical, of 59% after 8.0 min and 58% after 18.0 min of irradiation, with multiplicative correction factors *F* of 1.13 and 1.24, respectively. These acetaldehyde yields were verified to be consistent with those estimated by FT-IR analysis from residual spectra such as that shown in Figure 4D, and the acetaldehyde yield from this experiment is given in Table 1 in the column labeled "FT-IR". The PAN concentration profile for the experiments

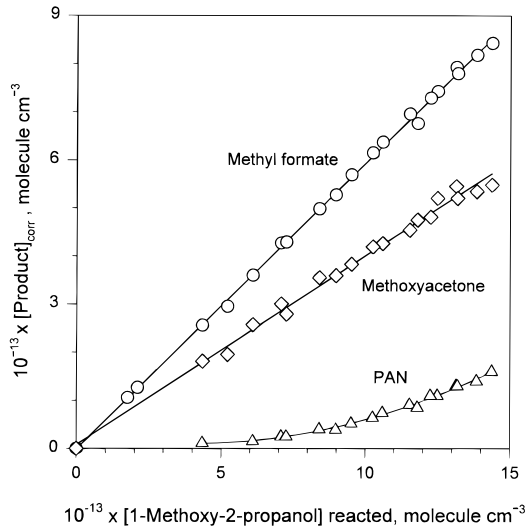

FIGURE 5. Plots of the amounts of products formed against the amounts of 1-methoxy-2-propanol reacted with OH radicals. The methyl formate and methoxyacetone concentrations have been corrected for secondary reactions with OH radicals. Analyses were by FT-IR spectroscopy.

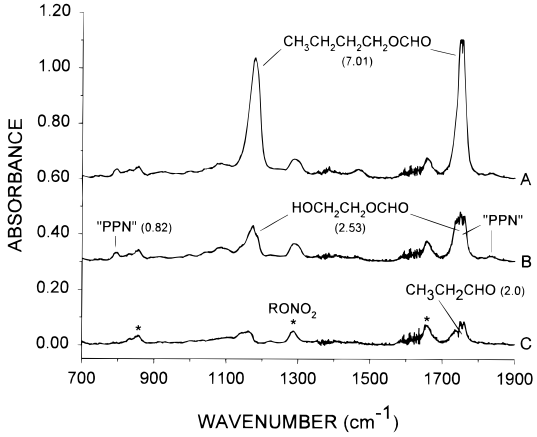

FIGURE 6. (A) Product spectrum from the photolysis of a 2-butoxyethanol−CH_3ONO−NO−air mixture after 29 min of irradiation and 50% conversion of the initial 2.51 × 10^{14} molecule cm^{-3} of 2-butoxyethanol, absorptions byproducts from CH_3ONO and NO subtracted, (B) after subtraction of absorptions by *n*-butyl formate, (C) after subtraction of absorptions by peroxypropionyl nitrate (PPN) and 2-hydroxyethyl formate. The numbers in parentheses are concentrations in units of 10^{13} molecule cm^{-3}. The absorption bands marked by an asterisk are attributed to organic nitrates, $RONO_2$ (see text).

summarized in Figure 5 show that PAN is formed as a result of secondary chemistry, with the measured PAN concentrations corresponding to a formation yield of 3−11% for the experimental conditions employed.

FT-IR spectroscopic analyses of irradiated CH_3ONO−NO−2-butoxyethanol−air mixtures showed the formation of *n*-butyl formate and 2-hydroxyethyl formate as the major products, as illustrated in Figure 6 (absorptions due to remaining reactants and to the products from the photooxidation of CH_3ONO and NO have been subtracted, as discussed above). Propanal was also observed as a product, but could only be measured by FT-IR analysis near the end of the photolysis when sufficiently high concentrations were present. Other products observed were organic nitrate(s) ($RONO_2$), as indicated by absorption bands very similar to those of *n*-propyl nitrate, and peroxyacyl nitrate(s), which could be mostly comprised of peroxypropionyl nitrate [$CH_3CH_2C(O)OONO_2$; PPN]. Estimates of $RONO_2$ concentrations were made from the integrated band area in the range 1255−1315 cm^{-1} (after subtraction of all identifiable species, including PPN) based on an average integrated absorption coefficient of 1.2 × 10^{-17} cm molecule^{-1} (base 10) from $RONO_2$ compounds (*16*). The analyses of PPN were based on the 1835 cm^{-1} absorption band but should be considered as upper limit estimates since they possibly include other peroxyacyl nitrates, hence the use of the label "PPN" in the following sections. The residual spectra contained other weak absorptions by an unidentified product(s), including a band(s) in the C═O stretch region (with some contribution from 3-hydroxybutyl formate) which remained after subtraction of absorptions by propanal (see API-MS analyses, below).

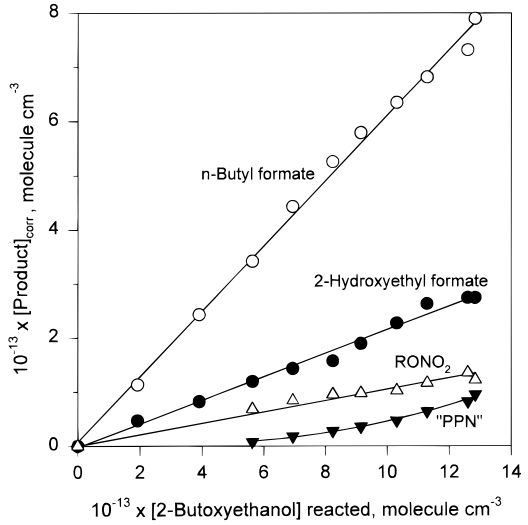

FIGURE 7. Plots of the amounts of products formed against the amounts of 2-butoxyethanol reacted with OH radicals. The *n*-butyl formate and 2-hydroxyethyl formate concentrations have been corrected for secondary reactions with OH radicals. Analyses were by FT-IR spectroscopy.

The amounts of *n*-butyl formate and 2-hydroxyethyl formate formed, corrected for secondary reactions with the OH radical, are plotted in Figure 7 against the amounts of 2-butoxyethanol reacted. A rate constant for reaction of the OH radical with 2-hydroxyethyl formate of 6.0 × 10^{-12} cm^3 molecule^{-1} s^{-1} was estimated (*27*) and used to correct for secondary reactions. For the 33-min experiment represented in Figure 7, the calculated maximum values of *F* were 1.05, 1.08, and 1.29 for *n*-butyl formate, 2-hydroxyethyl formate, and propanal, respectively. Least-squares analyses of the data shown in Figure 7 lead to the product formation yields shown in Table 1. The series of spectra recorded near the end of the irradiation enabled three measurements of the propanal concentration to be made, resulting in corrected propanal yields of 0.19−0.23, with an average of 0.21 (± 40% estimated uncertainty) [Table 1]. The $RONO_2$ yield has been estimated as 0.10 ± 0.03, and this is also given in Table 1. The plot of the measured "PPN" concentrations against the amounts of 2-butoxyethanol reacted (Figure 7) shows that "PPN" is formed as a result of secondary chemistry, with the measured "PPN" concentrations corresponding to a formation yield of 1−7% for the experimental conditions employed.

Teflon Chamber with Analyses by API-MS. Experiments were carried out using API-MS for analysis of the products formed from the reactions of the OH radical with 1-methoxy-2-propanol and 2-butoxyethanol in the presence of NO. API-MS/MS "daughter ion" and "parent ion" spectra were obtained for ion peaks observed in the API-MS analyses. Product ion peaks were identified based on the observation

TABLE 2. Products Formed from the Gas-Phase Reactions of the OH Radical with 1-Methoxy-2-propanol and 2-Butoxyethanol in the Presence of NO, As Observed by API-MS and API-MS/MS Analyses

product		API-MS data	other evidence
		1-Methoxy-2-propanol, M_{MP} (MW 90)	
methyl formate	M_1 (MW 60)	$M_1 + H = 61$	MS/MS of weak 61 u ion peak identical to that of authentic standard; parents of 61 u ion observed at 149 [$M_1 + M_2 + H$], 151 [$M_1 + M_{MP} + H$], and 181 [$M_1 + M_1 + M_1 + H$] u.
methoxyacetone	M_2 (MW 88)	$M_2 + H = 89$ $M_2 + M_{MP} + H = 179$ $M_2 + M_{MP} + H + H_2O = 197$ $M_2 + M_{MP} + H + 2H_2O = 215$	MS/MS of 89 u ion peak identical to that of authentic standard; MS/MS of 179 u ion peak; parents of 89 u ion observed at 177 [$M_2 + M_2 + H$], 179, 197, and 215 u.
		2-Butoxyethanol, M_{BE} (MW 118)	
n-butyl formate	M_1 (MW 102)	$M_1 + H = 103$	MS/MS of 103 u ion peak consistent with that of authentic standard; parents of 103 u ion observed at 161 [$M_1 + M_3 + H$], 205 [$M_1 + M_1 + H$], 221 [$M_1 + M_{BE} + H$], and 282 [$M_1 + M_4 + H$] u.
2-hydroxyethyl formate	M_2 (MW 90)	$M_2 + H = 91$	MS/MS of 91 u ion peak identical to that of synthesized standard; parents of 91 u ion observed at 149 [$M_2 + M_3 + H$], 181 [$M_2 + M_2 + H$], 193 [$M_2 + M_1 + H$], 209 [$M_2 + M_5 + H$], and 270 [$M_2 + M_4 + H$] u.
propanal	M_3 (MW 58)	$M_3 + H = 59$	parent of 59 u ion observed at 238 [$M_3 + M_4 + H$] u.
nitrate	M_4 (MW 179)	$M_4 + H = 180$ $M_4 + M_{BE} + H = 298$ $M_4 + M_5 + H = 312$	MS/MS of 180 u ion peak showing strong NO_2^+ fragment ion at 46 u; MS/MS of 298 u ion peak showing [$M_4 + H$] and [$M_{BE} + H$] ions.
$CH_3CH_2C(O)CH_2OCH_2CH_2OH$ or isomers	M_5 (MW 132)	$M_5 + H = 133$ $M_5 + M_{BE} + H = 251$ $M_5 + M_5 + H = 265$ $M_5 + M_4 + H = 312$	MS/MS of 133 u ion peak; parents of 133 u ion observed at 251, 265, 269 [$M_5 + M_{BE} + H + H_2O$], and 312 u.

of homo- or heterodimer ions (for example, $[(M_{P1})_2+H]^+$, $[(M_{P2})_2+H]^+$ and $[M_{P1}+M_{P2}+H]^+$, where P1 and P2 are products or the glycol ether reactants) in the API-MS/MS "parent ion" spectra, and consistency of the API-MS/MS "daughter ion" spectrum of a homo- or heterodimer ion with the "parent ion" spectra of the various $[M_P+H]^+$ ion peaks. Water cluster ion peaks of the product ions, $[M+H+H_2O]^+$, were also occasionally observed. The products observed are listed in Table 2 and the evidence for the formation of these products, in the form of API-MS and API-MS/MS data of molecular ions, dominant fragment ions, and the presence of homo- and heterodimers formed in the API-MS under the experimental conditions employed, is also summarized in Table 2.

The API-MS and API-MS/MS spectra obtained from the 1-methoxy-2-propanol reaction provided evidence for the formation of methyl formate and methoxyacetone (Table 2). Because the 45-u ion was a fragment of the API-MS/MS "daughter ion" spectrum of the 91 u $[M+H]^+$ ion of 1-methoxy-2-propanol and no obvious enhancement of the very weak 45 u ion peak was observed in the irradiated CH_3-ONO−NO−1-methoxy-2-propanol−air mixture compared to the unirradiated mixture, the formation of acetaldehyde could not be confirmed by these API-MS analyses. No evidence for the formation of other products was obtained from the API-MS and API-MS/MS analyses.

API-MS and API-MS/MS spectra of the 2-butoxyethanol reaction showed evidence for the formation of *n*-butyl formate, 2-hydroxyethyl formate, propanal, an organic nitrate of molecular weight 179, and a product of molecular weight 132 (Table 2) [note that 2-hydroxybutyl formate and 3-hydroxybutyl formate have the same molecular weight as 2-butoxyethanol]. The API-MS/MS spectra of the molecular weight 132 and 179 products are shown in Figure 8. The presence of a prominent NO_2^+ fragment ion at 46 u indicates that the product of molecular weight 179 is a nitrate of formula $C_6H_{13}NO_5$ [$CH_3CH_2CH_2CH(ONO_2)OCH_2CH_2OH$ and/or its isomers (see discussion below)].

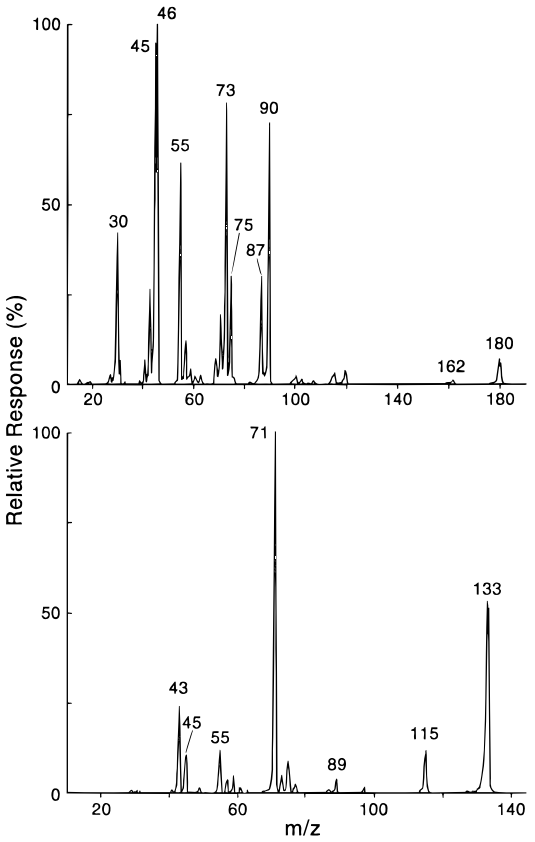

FIGURE 8. API-MS/MS CAD "daughter ion" spectra of the 180 u (top) and 133 u (bottom) ion peaks observed in the API-MS analyses of irradiated CH_3ONO−NO−2-butoxyethanol−air mixtures. The 46 u fragment ion in the API-MS/MS spectrum of the 180 u ion peak is attributed to NO_2^+.

The observation of ion peaks at 73, 101, 117, 189, and 283 u in the API-MS spectra suggests the presence of other products, although some of these ion peaks are fragments of $[M+H]^+$ ion peaks of the products M_1 through M_5 or of their homo- and heterodimers (for example, the 189 u ion peak was a weak fragment of the 251 u heterodimer). The ion peak at 73 u could be the $[M+H]^+$ of butanal, and an API-MS/MS spectrum of the 283 u ion peak suggested a heterodimer of 2-butoxyethanol and a product of molecular weight 164. However, no additional evidence in the form of homo- or heterodimers of these molecular weight species was obtained.

Discussion

1-Methoxy-2-propanol Reaction. The products observed by GC-FID, FT-IR spectroscopy, and API-MS analyses were methyl formate, methoxyacetone, and acetaldehyde. The formation yields of methyl formate and methoxyacetone measured by GC-FID and FT-IR analyses are in excellent agreement (Table 1), with formation yields of 0.59 ± 0.05 and 0.39 ± 0.04, respectively. As obvious from the data shown in Table 1, the measurements of the formation yield of acetaldehyde were less precise, but are totally consistent with acetaldehyde being a coproduct to methyl formate. The products observed are explained by reaction of the OH radical with 1-methoxy-2-propanol proceeding by H-atom abstraction from the C−H bonds of the >CH− and $-CH_2-$ groups:

$$OH + CH_3CH(OH)CH_2OCH_3 \rightarrow H_2O + CH_3\dot{C}(OH)CH_2OCH_3 \quad (4a)$$

$$OH + CH_3CH(OH)CH_2OCH_3 \rightarrow H_2O + CH_3CH(OH)\dot{C}HOCH_3 \quad (4b)$$

The α-hydroxy radical $CH_3\dot{C}(OH)CH_2OCH_3$ is expected to react with O_2 (*1, 28*) to form methoxyacetone:

$$CH_3\dot{C}(OH)CH_2OCH_3 + O_2 \rightarrow CH_3C(O)CH_2OCH_3 + HO_2 \quad (5)$$

The $CH_3CH(OH)\dot{C}HOCH_3$ radical adds O_2 to form a peroxy radical which, in the presence of NO, reacts to form an alkoxy radical plus NO_2 or an organic nitrate (*1*):

$$CH_3CH(OH)\dot{C}HOCH_3 + O_2 \rightarrow CH_3CH(OH)CH(OO^\bullet)OCH_3 \quad (6)$$

$$CH_3CH(OH)CH(OO^\bullet)OCH_3 + NO \rightarrow CH_3CH(OH)CH(O^\bullet)OCH_3 + NO_2 \quad (7a)$$

$$CH_3CH(OH)CH(OO^\bullet)OCH_3 + NO \rightarrow CH_3CH(OH)CH(ONO_2)OCH_3 \quad (7b)$$

This alkoxy radical formed in reaction 7a is expected to decompose (*1*), leading to the formation of methyl formate plus acetaldehyde:

$$CH_3CH(OH)CH(O^\bullet)OCH_3 \rightarrow CH_3OCHO + CH_3\dot{C}HOH \quad (8)$$

$$CH_3\dot{C}HOH \xrightarrow{O_2} CH_3CHO + HO_2$$

The sum of the methyl formate and methoxyacetone formation yields is 0.98 ± 0.07, showing that essentially all of the reaction pathways have been observed. Other initial reaction pathways (H-atom abstraction from the −OH or $-CH_3$ groups) and any formation of the organic nitrate $CH_3CH(OH)CH(ONO_2)OCH_3$ from reaction 7b must then account for ≤ 9% of the overall product yield. The structure−reactivity estimation method of Kwok and Atkinson (*27*) leads to calculated fractions of the OH radical reaction with 1-methoxy-2-propanol proceeding by H-atom abstraction from the $-OCH_3$, >CH−, $-CH_2-$, $-CH_3$, and −OH groups of 6%, 43%, 50%, <1%, and <1%, respectively. This prediction (*27*) of 43% and 50% of the overall reaction proceeding by initial H-atom abstraction from the >CH− and $-CH_2-$ groups, respectively, is in good agreement with respective percentages of 39% and 59% obtained from the products observed and their formation yields.

2-Butoxyethanol Reaction. The products observed by GC-FID, FT-IR spectroscopy, and API-MS analyses were *n*-butyl formate, 2-hydroxyethyl formate, propanal, 3-hydroxybutyl formate, an organic nitrate of molecular weight 179 (FT-IR and API-MS analyses), and a product of molecular weight 132 (API-MS analyses) which may account for part of the observed C−O stretch absorption in the FT-IR spectrum. The formation yields of *n*-butyl formate and propanal measured by GC-FID and FT-IR analyses are in excellent agreement (Table 1), with formation yields of 0.57 ± 0.05 and 0.21 ± 0.02, respectively. The formation yield of 2-hydroxyethyl formate is essentially identical to that of propanal, consistent with these two products being formed from the same initial reaction pathway.

The formation of the products *n*-butyl formate and propanal plus 2-hydroxyethyl formate accounts for 78 ± 6% of the overall reaction products (Table 1), suggesting that the major alkoxy radicals formed are $CH_3CH_2CH_2CH_2OCH(O^\bullet)CH_2OH$ and $CH_3CH_2CH_2CH(O^\bullet)OCH_2CH_2OH$. These two alkoxy radicals arise after H-atom abstraction from the two $-CH_2-$ groups adjacent to the ether linkage followed by reactions analogous to reactions 6 and 7a shown above for the $CH_3CH(OH)\dot{C}HOCH_3$ radical formed from the 1-methoxy-2-propanol reaction. The observed formation of the molecular weight 179 nitrate is consistent with formation from the reaction of the peroxy radicals $CH_3CH_2CH_2CH_2OCH(OO^\bullet)CH_2OH$ and/or $CH_3CH_2CH_2CH(OO^\bullet)OCH_2CH_2OH$ with NO [analogous to reaction 7b], although it should be noted that $RO_2^\bullet + NO$ reactions of all of the peroxy radicals formed after H-atom abstraction from the C−H bonds apart from those in the $-CH_2OH$ group can lead to the formation of a molecular weight 179 $C_6H_{13}NO_5$ nitrate.

The potential reactions of the $CH_3CH_2CH_2CH_2OCH(O^\bullet)CH_2OH$ and $CH_3CH_2CH_2CH(O^\bullet)OCH_2CH_2OH$ alkoxy radicals are shown in Schemes 1 and 2, respectively, where the products shown in boxes were identified and quantified and those underlined are consistent with the API-MS analyses (noting that the hemiacetal $CH_3CH_2CH_2CH(OH)OCH_2CHO$ in Scheme 2 may decompose to butanal plus glycolaldehyde during sampling and GC analysis or when protonated in the API-MS). The products formed, and their yields, from the reactions of the $CH_3CH_2CH_2CH_2O^\bullet$ radical (Scheme 1) and the $HOCH_2CH_2O^\bullet$ radical (Scheme 2) in air are based on literature data (*1, 28, 29*).

The products observed are in agreement with the decomposition pathway

$$RCH(O^\bullet)OR' \rightarrow R^\bullet + R'OCHO \quad (9)$$

shown in Schemes 1 and 2 dominating over the alternative decomposition pathway,

$$RCH(O^\bullet)OR' \rightarrow RCHO + R'O^\bullet \quad (10)$$

for both the $CH_3CH_2CH_2CH_2OCH(O^\bullet)CH_2OH$ and $CH_3CH_2CH_2CH(O^\bullet)OCH_2CH_2OH$ radicals, and this is confirmed by our measured upper limit to the butanal formation yield of <0.01 (Table 1).

SCHEME 1

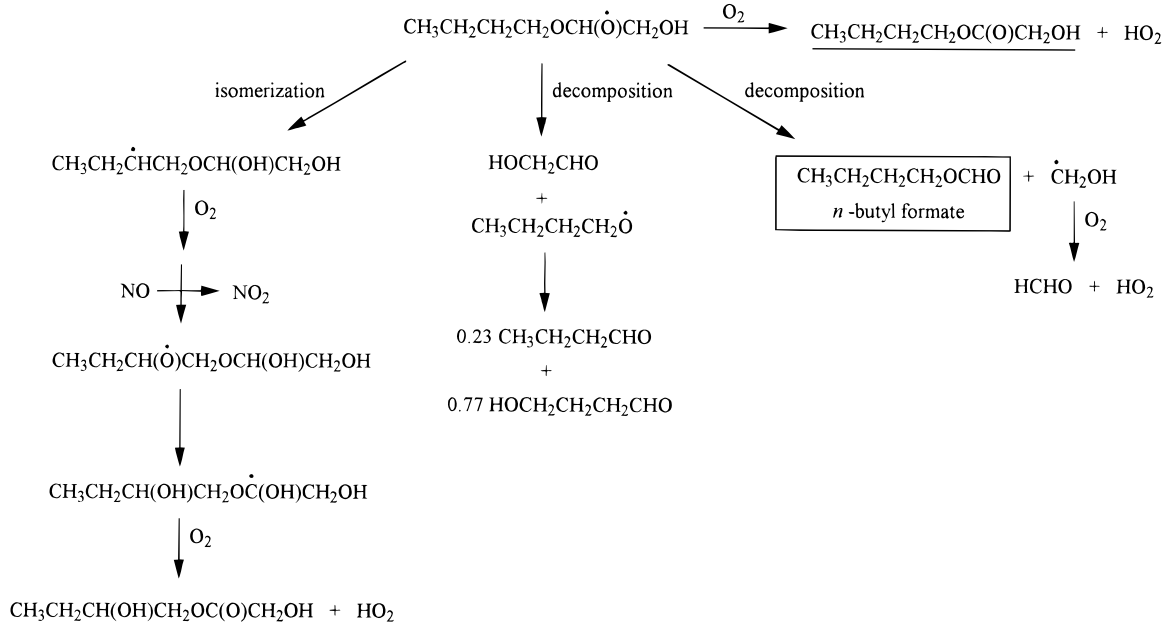

SCHEME 2

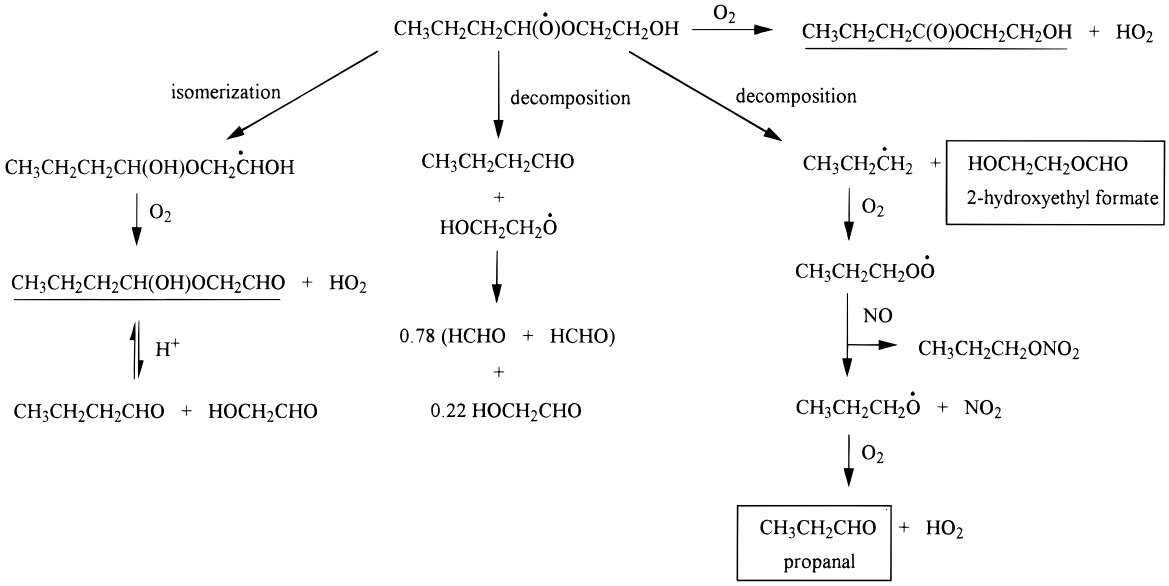

The formation route to 3-hydroxybutyl formate must involve initial H-atom abstraction to form the $CH_3\dot{C}HCH_2CH_2OCH_2CH_2OH$ radical, which then (after addition of O_2 and reaction with NO) leads to the $CH_3CH(O^\bullet)CH_2CH_2OCH_2CH_2OH$ radical, which must then isomerize through a seven-membered transition state (*15*):

$$CH_3CH(O^\bullet)CH_2CH_2OCH_2CH_2OH \rightarrow CH_3CH(OH)CH_2CH_2O\dot{C}HCH_2OH \quad (11)$$

This isomerization via a seven-membered transition state must be competitive with the reaction with O_2 [to yield $CH_3C(O)CH_2CH_2OCH_2CH_2OH$ plus the HO_2 radical] and with decomposition (to yield CH_3CHO plus, presumably, ultimately $HOCH_2CH_2OCH_2CHO$).

Addition of O_2 to the $CH_3CH(OH)CH_2CH_2O\dot{C}HCH_2OH$ radical and reaction with NO (analogous to reactions 6 and 7a shown above) results in the $CH_3CH(OH)CH_2CH_2OCH(O^\bullet)CH_2OH$ β-hydroxyalkoxy radical, which can decompose to form 3-hydroxybutyl formate (*15*):

$$CH_3CH(OH)CH_2CH_2OCH(O^\bullet)CH_2OH \rightarrow CH_3CH(OH)CH_2CH_2OCHO + \dot{C}H_2OH \quad (12)$$

$$\dot{C}H_2OH \xrightarrow{O_2} HCHO + HO_2$$

The structure−reactivity estimation method of Kwok and Atkinson (*27*) predicts that the percentages of the overall OH radical reaction arising from H-atom abstraction from the C−H bonds in $CH_3CH_2CH_2CH_2OCH_2CH_2OH$ are (for the carbons as written from left to right) <1%, 4%, 5%, 37%, 37%, and 15%, with <1% H-atom abstraction from the O−H bond. Our product data show that H-atom abstraction from the $-CH_2-$ groups adjacent to the ether linkage dominates (in agreement with the above predictions), and accounts for

~23% abstraction from the italicized $-CH_2-$ group in $CH_3CH_2CH_2\mathit{CH_2}OCH_2CH_2OH$ and ~63% abstraction from the italicized $-CH_2-$ group in $CH_3CH_2CH_2CH_2O\mathit{CH_2}CH_2OH$ (assuming that organic nitrate formation occurs from the various $RO_2^\bullet + NO$ reactions with the same yield). Our data indicate that the $-CH_2-$ group with $-O-$ and $-CH_2OH$ substituents is activated over the $-CH_2-$ group with $-O-$ and $-C_3H_7$ substituents.

No evidence was obtained from the GC or API-MS analyses (and FT-IR analyses were not specific) for the presence of $CH_3CH_2CH_2CH_2OCH_2CHO$, the expected product formed after H-atom abstraction from the C−H bonds in the $-CH_2OH$ group:

$$CH_3CH_2CH_2CH_2OCH_2\dot{C}HOH + O_2 \rightarrow CH_3CH_2CH_2CH_2OCH_2CHO + HO_2 \quad (13)$$

As discussed above, 3-hydroxybutyl formate must arise from H-atom abstraction from the C−H bonds of the carbon γ to the ether oxygen, while the expected products formed after H-atom abstraction from the C−H bonds of the carbon β to the ether oxygen are (by analogous reactions to those discussed above for the formation of 3-hydroxybutyl formate) 2-hydroxybutyl formate (isomerization reaction, and with a measured formation yield of <3%), $CH_3CH_2C(O)CH_2OCH_2CH_2OH$ (O_2 reaction, formation consistent with our API-MS analyses), and propanal plus 2-hydroxyethyl formate or CH_3CHO plus $HOCH_2CH_2OCH_2CHO$ (decomposition reaction).

As shown in Scheme 2 and noted above, propanal is formed as a coproduct to 2-hydroxyethyl formate, via the intermediary of the 1-propyl radical. After addition of O_2, the $CH_3CH_2CH_2OO^\bullet$ radical reaction with NO leads to the formation of 2% 1-propyl nitrate and 98% 1-propoxy radical plus NO_2 (*30*), with the 1-propoxy radical reacting with O_2 to form propanal (*1*, *28*, *29*). The formation yields of *n*-butyl formate (plus HCHO coproduct), 3-hydroxybutyl formate (plus the expected HCHO coproduct) and 2-hydroxyethyl formate plus propanal, combined with the measured formation yield of the nitrate (presumed to be largely the $C_6H_{13}NO_5$ nitrate observed by the API-MS analyses), account for 96 ± 7% of the reaction pathways. Other reaction pathways, leading to products such as molecular weight 132 hydroxyesters and hydroxycarbonyl-ethers $CH_3CH_2CH_2CH_2OC(O)CH_2OH$ (Scheme 1), $CH_3CH_2CH_2C(O)OCH_2CH_2OH$ (Scheme 2), $CH_3CH_2CH_2CH(OH)OCH_2CHO$ (Scheme 2), $CH_3CH_2C(O)CH_2OCH_2CH_2OH$, or $CH_3C(O)CH_2CH_2OCH_2CH_2OH$, must then occur to a minor extent (<11%). The formation of $C_6H_{12}O_3$ hydroxyesters and/or hydroxycarbonyl ethers would be consistent with both the API-MS and FT-IR analyses (see above).

The products of the OH radical-initiated reaction of 2-butoxyethanol in the presence of NO have been previously studied by Stemmler et al. (*15*). The products identified and quantified by Stemmler et al. (*15*) which we observed were (our product yields are given in parentheses) *n*-butyl formate, 0.35 ± 0.11 (0.57 ± 0.05); propanal, ~0.2−0.3 (0.21 ± 0.02); 2-hydroxyethyl formate, 0.39 ± 0.18 (0.22 ± 0.05); 3-hydroxybutyl formate, ~0.20 (0.07 ± 0.03); 2-hydroxybutyl formate [$CH_3CH_2CH(OH)CH_2OCHO$], ~0.05 (<0.03); $CH_3CH_2CH_2C(O)OCH_2CH_2OH$, ~0.02−0.03 (consistent with our API-MS and FT-IR analyses, see above); and butanal, <0.011 (<0.01). In addition, Stemmler et al. (*15*) observed the following products which were not observed in our study, these being butoxyacetaldehyde [$CH_3CH_2CH_2CH_2OCH_2CHO$], 0.12 ± 0.09; 2-propyl-1,3-dioxalane, 0.025 ± 0.005; and 1-propyl nitrate, 0.038 ± 0.018. Obviously, there are areas of broad agreement and some disagreements. The major disagreements are in the formation yields of *n*-butyl formate, 2-hydroxyethyl formate, and 3-hydroxybutyl formate measured in the two studies, noting that the quantification of 3-hydroxybutyl formate by Stemmler et al. (*15*) was stated to be subject to significant uncertainties. The other products observed by Stemmler et al. (*15*), but not by us, have relatively low formation yields and, together with $CH_3CH_2CH_2C(O)OCH_2CH_2OH$ (or its isomers), may contribute to the 4 ± 7% of products/reaction pathways not accounted for in our study. Because we have identified and quantified the majority of the reaction products and reaction pathways involved in the OH radical-initiated reaction of 2-butoxyethanol, and have identified 96 ± 7% of the reaction pathways, no significant products or reaction pathways are unaccounted for.

The product and mechanistic data obtained here for the reactions of the OH radical with 1-methoxy-2-propanol and 2-butoxyethanol in the presence of NO account for all or almost all of the reaction products and pathways. These data can now be used in detailed chemical mechanisms for the photooxidations of these compounds in ambient air and will contribute to the accurate calculation of their ozone-forming potentials (*5*).

Acknowledgments

The authors gratefully thank the Chemical Manufacturers' Association, Ethylene Glycol Ethers Panel, for supporting this research through Contract EGE-73.0-VOC-ATKIN.

Literature Cited

(1) Atkinson, R. *J. Phys. Chem. Ref. Data* **1994**, *Monograph 2*, 1−216.
(2) Atkinson, R. Gas-Phase Tropospheric Chemistry of Organic Compounds, In *Volatile Organic Compounds in the Atmosphere*; Issues in Environmental Science and Technology, 4; The Royal Society of Chemistry: Cambridge, UK, 1995; pp 65−89.
(3) Solvents. In *Handbook of Environmental Fate and Exposure Data for Organic Solvents*; Howard, P. H., Ed.; Lewis Publishers: Chelsea, MI, 1990; Vol. II.
(4) Solvents 2. In *Handbook of Environmental Fate and Exposure Data for Organic Solvents*; Howard, P. H., Ed.; Lewis Publishers: Chelsea, MI, 1993; Vol. IV.
(5) Carter, W. P. L. *J. Air Waste Manag. Assoc.* **1994**, *44*, 881−899.
(6) Weidelmann, A.; Zetzsch, C. Presented at Bunsentagung, Ulm und Neu-Ulm, May 20−22, 1982; cited in ref 23.
(7) Hartmann, D.; Gedra, A.; Rhäsa, D.; Zellner, R. *Rate Constants for Reaction of OH Radicals with Acetates and Glycols in the Gas Phase*, In *Physico-Chemical Behaviour of Atmospheric Pollutants*; D. Reidel Publishing Co., Dordrecht, The Netherlands, 1987; pp 225−235.
(8) Dagaut, P.; Liu, R.; Wallington, T. J.; Kurylo, M. J. *J. Phys. Chem.* **1989**, *93*, 7838−7840.
(9) Neavyn, R.; Sidebottom, H.; Treacy, J. Reactions of Hydroxyl Radicals with Polyfunctional Group Oxygen-Containing Organic Compounds. In *The Proceedings of EUROTRAC Symposium '*94; Borrell, P. M., Borrell, P., Cvitaš, T., Seiler, W., Eds.; SPB Academic Publishing Bv: The Hague, The Netherlands, 1994; pp 105−109.
(10) Stemmler, K.; Kinnison, D. J.; Kerr, J. A. *J. Phys. Chem.* **1996**, *100*, 2114−2116.
(11) Porter, E.; Wenger, J.; Treacy, J.; Sidebottom, H.; Mellouki, A.; Téton, S.; LeBras, G. *J. Phys. Chem. A* **1997**, *101*, 5770−5775.
(12) Aschmann, S. M.; Atkinson, R. *Int. J. Chem. Kinet.* **1998**, *30*, 533−540.
(13) Chew, A. A.; Atkinson, R.; Aschmann, S. M. *J. Chem. Soc., Faraday Trans.* **1998**, *94*, 1083−1089.
(14) Stemmler, K.; Mengon, W.; Kerr, J. A. *Environ. Sci. Technol.* **1996**, *30*, 3385−3391.
(15) Stemmler, K.; Mengon, W.; Kinnison, D. J.; Kerr, J. A. *Environ. Sci. Technol.* **1997**, *31*, 1496−1504.
(16) Tuazon, E. C.; Atkinson, R. *Int. J. Chem. Kinet.* **1990**, *22*, 1221−1236.
(17) Atkinson, R.; Tuazon, E. C.; Aschmann, S. M. *Environ. Sci. Technol.* **1995**, *29*, 1674−1680.
(18) Tuazon, E. C.; Aschmann, S. M.; Arey, J.; Atkinson, R. *Environ. Sci. Technol.* **1997**, *31*, 3004−3009.
(19) Aschmann, S. M.; Chew, A. A.; Arey, J.; Atkinson, R. *J. Phys. Chem. A* **1997**, *101*, 8042−8048.
(20) Taylor, W. D.; Allston, T. D.; Moscato, M. J.; Fazekas, G. B.; Kozlowski, R.; Takacs, G. A. *Int. J. Chem. Kinet.* **1980**, *12*, 231−240.
(21) Stephens, E. R. *Anal. Chem.* **1964**, *36*, 928−929.

(22) Scanlon, J. T.; Willis, D. E. *J. Chromat. Sci.* **1985**, *23*, 333−340.
(23) Atkinson, R. *J. Phys. Chem. Ref. Data* **1989**, *Monograph 1*, 1−246.
(24) Atkinson, R.; Aschmann, S. M.; Carter, W. P. L.; Winer, A. M.; Pitts, J. N., Jr. *J. Phys. Chem.* **1982**, *86*, 4563−4569.
(25) Wallington, T. J.; Dagaut, P.; Liu, R.; Kurylo, M. J. *Int. J. Chem. Kinet.* **1988**, *20*, 177−186.
(26) Le Calvé, S.; Le Bras, G.; Mellouki, A. *J. Phys. Chem. A* **1997**, *101*, 5489−5493.
(27) Kwok, E. S. C.; Atkinson, R. *Atmos. Environ.* **1995**, *29*, 1685−1695.
(28) Atkinson, R. *J. Phys. Chem. Ref. Data* **1997**, *26*, 215−290.
(29) Atkinson, R. *Int. J. Chem. Kinet.* **1997**, *29*, 99−111.
(30) Carter, W. P. L.; Atkinson, R. *J. Atmos. Chem.* **1989**, *8*, 165−173.

Received for review May 4, 1998. Revised manuscript received August 3, 1998. Accepted August 4, 1998.

ES980455C